

## Auger ionization in armchair-edge graphene nanoribbons

S. Konabe,<sup>1,2,\*</sup> N. Onoda,<sup>3</sup> and K. Watanabe<sup>3</sup>

<sup>1</sup>Graduate School of Pure and Applied Sciences, University of Tsukuba, Tsukuba, Ibaraki 305-8571, Japan

<sup>2</sup>CREST, Japan Science and Technology Agency, 5 Sanbancho, Chiyoda, Tokyo 102-0075, Japan

<sup>3</sup>Department of Physics, Faculty of Science, Tokyo University of Science, 1-3 Kagurazaka, Shinjuku, Tokyo 162-8601, Japan

(Received 1 April 2010; revised manuscript received 13 July 2010; published 6 August 2010)

Free electron-hole (e-h) pair generation from excitons in armchair-edged graphene nanoribbons (AGNRs) is theoretically investigated. We consider the generation of free e-h pairs by the Auger ionization of exciton-exciton scattering. We calculate e-h pair-generation times in a tight-binding approximation and found that the times were of picosecond order for 1.2–2.5-nm-wide ribbons due to efficient scattering between excitons. Additionally, the environmental effects are found to largely influence the Auger ionization process. Our calculations reveal the important role of the Auger ionization of excitons in AGNRs. These findings are of crucial importance for the application of AGNRs to photoelectronic and optoelectronic devices.

DOI: [10.1103/PhysRevB.82.073402](https://doi.org/10.1103/PhysRevB.82.073402)

PACS number(s): 78.67.Ch, 71.35.–y

### I. INTRODUCTION

The recent successful production of isolated single-layer nanometer-sized graphene, i.e., graphene nanoribbons (GNRs), has generated new interest in one-dimensional physics and provided novel building blocks for next generation devices.<sup>1–4</sup> Reflecting the quasi-one-dimensional structure of GNRs, many-body effects due to enhanced Coulomb interaction by the confined geometry greatly influence the energy band gap, giving a large self-energy correction.<sup>5</sup> Furthermore, effects beyond the one-particle excitation strongly influence the optical properties of GNRs. In fact, state-of-the-art *ab initio* calculations using the GW approximation and the Bethe-Salpeter equation demonstrated that excitonic effects are dominant in the absorption spectra of armchair-edged GNRs (AGNRs).<sup>6,7</sup>

From a technological point of view, direct band-gap AGNRs are desirable for the generation or detection of light and are a potential candidate for nanoscale optoelectric devices. However, the effectively enhanced Coulomb interaction could induce an efficient nonradiative recombination decay due to interactions between excitons. In semiconducting carbon nanotubes (CNTs), which are similar quasi-one-dimensional materials, exciton-exciton scattering occurs under high-intensity laser irradiation, leading to rapid recombination of excitons.<sup>8–13</sup> This nonradiative process, called Auger recombination between two excitons, is also expected to be efficient in AGNRs. While the existence of such rapid nonradiative recombination paths is an obstacle for light-emitting device applications, the Auger process would involve a simultaneous exciton ionization, called Auger ionization. It is thus important and necessary to study Auger recombination and ionization in AGNRs to enable device applications.

In this Brief Report, we report a theoretical study of free electron-hole (e-h) pair generation from excitons. As a mechanism of free e-h pair generation, we investigate the Auger ionization process between two excitons in AGNRs. We first calculate the excitonic states by solving the Bethe-Salpeter equation under the tight-binding approximation. We then calculate the Auger ionization rate for several widths of

AGNRs. Finally, we will discuss the environmental effects on free e-h pair generation. Present study elucidates a key role of Auger nonradiative recombination process in realizing AGNR-optoelectronic devices.

### II. EXCITONS IN AGNRs

The excitonic states in AGNRs are calculated under the tight-binding approximation. Noninteracting electronic states of AGNRs are obtained by imposing a fixed boundary condition on the eigenstates of graphene along the direction perpendicular to the ribbon axis. In this procedure, we do not take into account the effects of the spin degrees of freedom or of passivated hydrogen atoms. These effects are extensively studied by *ab initio* calculations.<sup>5–7,14</sup>

The quasiparticle band energies  $\varepsilon_{\mathbf{k}_c}$  and  $\varepsilon_{\mathbf{k}_v}$  for conduction and valence electrons are calculated using the random-phase approximation. The wave function of the quasiparticle (hole) is given by the tight-binding approximation as<sup>15</sup>

$$|\mathbf{k}_{c(v)}\rangle = \frac{1}{\sqrt{N_{\text{cell}}}} \sum_{\alpha=A,B} \sum_{i=1}^{N_{\text{cell}}} C_{\alpha}^{c(v)}(\mathbf{k}) e^{i\mathbf{k}\cdot\mathbf{R}_{\alpha,i}} |\phi(\mathbf{r}-\mathbf{R}_{\alpha,i})\rangle, \quad (1)$$

where  $N_{\text{cell}}$  is the total number of graphene unit cells in CNTs,  $C_{\alpha}^{c(v)}(\mathbf{k})$  the wave function coefficient for  $\alpha=A(B)$  site, and  $|\phi(\mathbf{r}-\mathbf{R}_{\alpha,i})\rangle$  is the atomic wave function. The electron-hole bound state,  $|\Phi_{\mathbf{q}}^n\rangle$ , is represented by the superposition of free e-h pair states,  $|\mathbf{k}_c, \mathbf{k}_v\rangle$ , with the weight  $\Psi_{\mathbf{k}_c, (\mathbf{k}-\mathbf{q})_v}^n$  as

$$|\Phi_{\mathbf{q}}^n\rangle = \sum_{\mathbf{k}} \sum_{c,v} \Psi_{\mathbf{k}_c, (\mathbf{k}-\mathbf{q})_v}^n |\mathbf{k}_c, \mathbf{k}_v\rangle, \quad (2)$$

where  $c$  and  $v$  refer to the conduction band and valence band, respectively. Here, we include only the lowest conduction and highest valence bands formed by the  $p_z$  orbitals. The  $n$ th ( $n=1, 2, \dots$ ) excitonic states with amplitude  $\Psi_{\mathbf{k}_c, (\mathbf{k}-\mathbf{q})_v}^n$  and energy  $E_{\mathbf{q}}^n$  satisfy the following Bethe-Salpeter equation:<sup>15–19</sup>

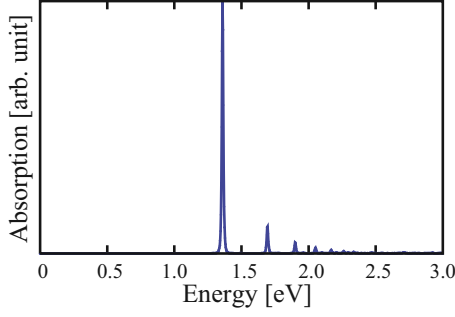


FIG. 1. (Color online) Absorption spectra of 18 AGNRs calculated by Eq. (4). The dielectric function,  $\kappa=5.0$ , and a broadening of 10 meV are chosen.

$$(\varepsilon_{k_c} - \varepsilon_{k_v})\Psi_{k_c, k_v}^n + \sum_{k'_c, k'_v} K_{k'_c, k'_v; k_c, k_v} \Psi_{k'_c, k'_v}^n = E_{\mathbf{q}}^n \Psi_{k_c, k_v}^n, \quad (3)$$

where  $K_{k'_c, k'_v; k_c, k_v}$  is the Coulomb interaction kernel that consists of the exchange and screened-direct terms. For the Coulomb potential between  $\pi$  orbitals, we employed the Ohno potential  $V(\mathbf{r}) = U/\kappa \sqrt{(\frac{4\pi\epsilon_0}{e^2} U|\mathbf{r}|)^2 + 1}$  with  $U = 11.3$  eV.<sup>15,17,19</sup> The screening by  $\sigma$  bands and by the surrounding environment is expressed by the dielectric constant  $\kappa$ .<sup>15,16</sup> The wave vector consists of the linear momentum  $k$  and subbands  $l$ , i.e.,  $\mathbf{k}=(k, l)$  due to the fixed boundary conditions.

From a solution of the Bethe-Salpeter Eq. (3), the absorption spectra is calculated from the following relation:

$$\alpha(\hbar\omega) = \frac{\pi\hbar^3}{e^2\varepsilon_0 c} \sum_n \left| \sum_{k_c, k_v} \frac{\Psi_{k_c, k_v}^n D_{k_c, k_v}}{E_0^1} \right|^2 \delta(\hbar\omega - E_0^n), \quad (4)$$

where  $D_{k_c, k_v} = \langle \mathbf{k}_c | z | \mathbf{k}_v \rangle$  is the dipole-matrix element between the conduction and valence bands. The light polarization axis is set to be parallel to the GNRs axes,  $z$  direction. This is because the optical absorption of a laser beam is greatest for this polarization configuration. The delta function in Eq. (4) is broadened by 10 meV. Figure 1 shows the absorption spectra for 18-AGNRs, where 18 refers to the number of bonds along the direction perpendicular to the ribbon axis. For the dielectric constant, we set  $\kappa=5.0$ . This value is selected since the Auger ionization does not occur below around  $\kappa=5.0$ , which will be discussed in Sec. III B. The van Hove-type spectral shape inherent to the one-dimensional structure changes to symmetrical peaks. This is the manifestation of excitonic effects in the photoresponse of AGNRs.

Figure 2 shows binding energies of excitons for 1.2–2.5-nm-wide ribbons. The binding energy decreases with increasing width of the AGNRs. This behavior should be compared with semiconducting CNTs,<sup>20,21</sup> where the binding energy decreases with increasing CNT diameter. A recent experiment enables the fabrication of AGNRs 2 nm wide.<sup>3</sup> At this width, the binding energy is calculated as 1.2–1.3 eV, and excitonic effects dominate the optical response at room temperature. Our calculations agree with the results of *ab initio* methods.<sup>5,7</sup>

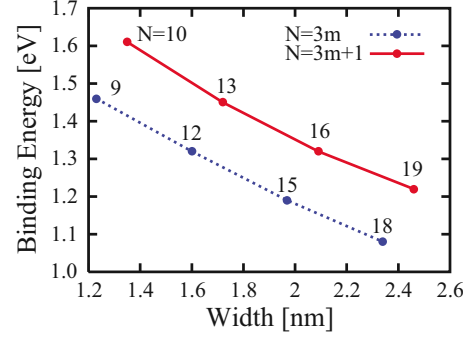


FIG. 2. (Color online) Binding energy of excitons for several widths of ribbon. Red (solid) and blue (dotted) lines represent  $N=3m+1$  and  $N=3m$  families, respectively.

### III. ELECTRON-HOLE PAIR-GENERATION RATES IN AGNRs

#### A. Auger ionization process in AGNRs

Next, let us show the e-h pair-generation rates by the Auger ionization process. When the high-intensity laser is irradiated creating more than two excitons, the Coulomb interaction makes the excitons recombine nonradiatively by transferring the energy of one exciton to the other exciton. The Auger recombination process is dominant when the Auger rate is larger than the other nonradiative recombination processes, such as exciton-phonon interaction.<sup>22</sup> For CNTs, the Auger recombination plays an important role above the laser intensity  $\sim 20$  pJ for 1  $\mu\text{m}$  long.<sup>23</sup> When one exciton has a sufficient energy to dissociate the other exciton into a free e-h pair, the exciton is ionized, called the Auger ionization.

Using the excitonic states derived in the previous section, we evaluate the free e-h pair-generation rates using Fermi's golden rule. For the free e-h pair generation, the following Auger ionization process of exciton-exciton scattering is considered. The lowest bright excitons in an initial state with momentum  $\mathbf{K}=\mathbf{0}$  and  $\mathbf{P}=\mathbf{0}$  interact with each other to become a free e-h pair as a final state. (We consider only the bright exciton that is directly excited by laser irradiation as the initial state. The influence of the dark excitons on the Auger process is not considered here.) Note that excitons generated by the absorption of a photon have approximate wave vectors  $\mathbf{K}=\mathbf{P}=\mathbf{0}$ . Regarding exciton dynamics, there has been no works in GNRs so far. For CNTs, there is a controversy on whether the annihilation process is a diffusion limited or coherent multiexciton process.<sup>24–30</sup> Therefore, our calculations for AGNRs assume that the generated excitons equilibrated very rapidly, and that the annihilation process is determined by the rates of scattering between two equilibrated excitons. In this process, the scattering occurs right after two excitons are generated, neglecting the exciton diffusion dynamics.<sup>26,31</sup> Through the above consideration, the Auger ionization rate between two excitons,  $\Gamma_{\mathbf{K}, \mathbf{P}}$  is given by<sup>32,33</sup>

$$\Gamma_{\mathbf{K}, \mathbf{P}} = \frac{2\pi}{\hbar} \sum_{k_c, k_v} |M|^2 \delta(E_{\mathbf{K}}^1 + E_{\mathbf{P}}^1 - \varepsilon_{k_c} - \varepsilon_{k_v}), \quad (5)$$

where  $E_{\mathbf{K}(\mathbf{P})}^1$  is the lowest exciton energy of the momentum  $\mathbf{K}(\mathbf{P})$  and  $\varepsilon_{k_c(k_v)}$  is the renormalized conduction- (valence-)

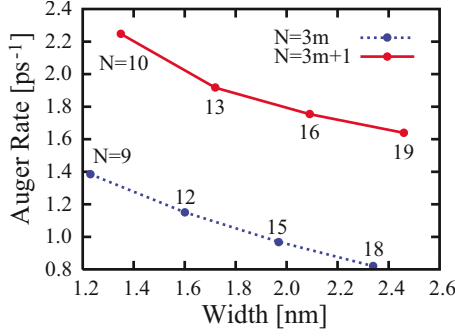


FIG. 3. (Color online) Nonradiative Auger recombination rates of 1- $\mu\text{m}$ -long AGNRs of several widths. As in Fig. 2, red (solid) and blue (dotted) lines represent  $N=3m+1$  and  $N=3m$  families, respectively.

band energy, corrected by the random-phase approximation. The matrix element of the Auger process  $M \equiv \langle \Psi_f | V | \Psi_i \rangle = M_1 - M_2$ , where the initial state is two bright excitons with zero momentum  $|\Psi_i\rangle = |\Phi_{\mathbf{K}=0}^1\rangle |\Phi_{\mathbf{P}=0}^1\rangle$  and the final state a free e-h pair  $|\Psi_f\rangle = |\mathbf{k}_c, \mathbf{k}_v\rangle$ , is expressed as

$$M_1 = \sum_{\mathbf{q}} \Psi_0^1(\mathbf{q}) \Psi_0^1(\mathbf{k}_v) \delta_{\mathbf{k}_c, \mathbf{k}_v} \times \sum_{s', s} C_{s'}^{c*}(\mathbf{k}_c) C_{s'}^c(\mathbf{q}) C_s^c(\mathbf{k}_v) C_s^{v*}(\mathbf{q}) v_{s', s}(\mathbf{k}_c - \mathbf{q}), \quad (6)$$

$$M_2 = \sum_{\mathbf{q}} \Psi_0^1(\mathbf{q}) \Psi_0^1(\mathbf{k}_v) \delta_{\mathbf{k}_c, \mathbf{k}_v} \times \sum_{s', s} C_{s'}^{c*}(\mathbf{k}_c) C_{s'}^c(\mathbf{q}) C_s^c(\mathbf{k}_v) C_s^{v*}(\mathbf{q}) v_{s', s}(\mathbf{k}_v - \mathbf{q}). \quad (7)$$

In Eqs. (6) and (7),  $C_s^{(v)}(\mathbf{q})$  is the wave-function coefficient given in Eq. (1) and  $v_{s', s}(\mathbf{q})$  is the Fourier transform of the Coulomb interaction. The subscript  $s(s')$  indicates two carbon atoms in the graphene unit cell.

The e-h pair-generation rates of AGNRs 1.2–2.5 nm wide for  $\kappa=5.0$  are shown in Fig. 3. Within this range of widths, the e-h pair-generation times are of picosecond order. From Fig. 3, we found the following interesting features. First, the e-h generation rates depend on the family type, i.e.,  $N=3m$  or  $N=3m+1$ , of the AGNRs. This behavior originates from the dependence of the binding energy on the family type (see Fig. 2). Second, these rates decrease with increasing width of AGNRs because the binding energy of an exciton decreases.<sup>33</sup> For experimentally accessible sizes of AGNRs, i.e., 2 nm wide, our calculation shows that the e-h pairs generation rate is a few per picosecond while the radiative recombination rate is estimated as a few per nanosecond. Therefore the Auger ionization process should be effective under high-intensity laser irradiation when many excitons are present. As mentioned above, for CNTs,<sup>23</sup> the required laser intensity for the Auger process is estimated as  $\sim 20$  pJ for 1  $\mu\text{m}$  long. Although there has been no experiment of the Auger process in GNRs, we assume that the required laser intensity for GNRs is comparable to CNTs.

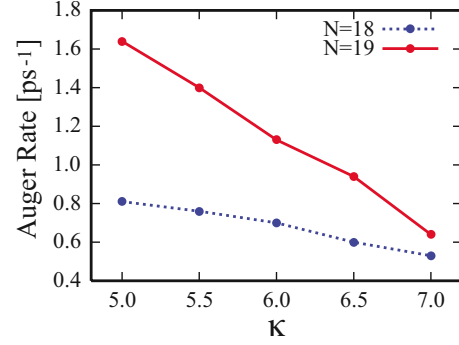


FIG. 4. (Color online) Environmental effects on Auger ionization rates. Below  $\kappa=5.0$ , Auger ionization did not occur.

### B. Environmental effects on Auger ionization

In this section, we discuss environmental effects represented by the dielectric constant  $\kappa$  on the free e-h pair-generation rates. In Fig. 4, we plot the  $\kappa$  dependence of the e-h pair-generation rates for 18- and 19-AGNRs. Our calculation shows that the e-h pair generation by the Auger ionization process is largely influenced by environmental effects through the  $\kappa$  dependence of the Coulomb interaction.

To generate free e-h pairs, the exciton-exciton interaction must be sufficiently large to dissociate an exciton into a free e-h pair. It is expected that low  $\kappa$  (i.e., less screening) leads to efficient generation of free e-h pairs since the Auger ionization rate is determined by the matrix elements of the Coulomb interaction, which is controlled by  $\kappa$ . However, the dissociation process of an exciton to a free e-h pair is not allowed by the energy conservation if the binding energy of an exciton is larger than the exciton energy. The threshold value of  $\kappa$  is considered to depend on the ribbon width.

## IV. SUMMARY

In summary, we studied e-h pair generation from excitons by the Auger ionization of two excitons in AGNRs. The e-h pair-generation rates of several widths of AGNRs were calculated under the tight-binding approximation. We found that the ionization times (inverse of generation rates) were very fast, of picosecond order, because of the enhanced Coulomb interaction in quasi-one-dimensional structures. We also showed that e-h pair generation is largely influenced by environmental effects and is unlikely to occur below a threshold value of  $\kappa$ , which depends on the ribbon width.

Our free e-h pair generation findings could be observed experimentally by femtosecond pump-probe spectroscopy, as performed on CNTs (Refs. 23 and 34) or by photocurrent spectroscopy, although it is challenging to suspend AGNRs between bridges. We consider that the present annihilation process by two equilibrated excitons is a reasonable assumption and expect that future experiments support the present mechanism.

In the application of AGNRs in light-emitting devices, the rapid nonradiative Auger decay rates are a severe obstacle. However, we emphasize that efficient Auger ionization can be used to generate sufficient carriers from excitons. Thus,

the Auger ionization process in AGNRs also provides a novel route to the application of AGNRs to photoconductive devices.

#### ACKNOWLEDGMENTS

The authors thank Daisuke Hirai for fruitful discussions.

This work was partly supported by CREST in the Japan Science and Technology Agency and a Grant-in-Aid for Scientific Research from the Ministry of Education, Culture, Sports, Science and Technology of Japan. K.W. acknowledges partial financial support through a Grant-in-Aid (Grant No. 19540411) from the Ministry of Education, Culture, Sports, Science and Technology (MEXT).

\*konabe@comas.frsc.tsukuba.ac.jp

- <sup>1</sup>M. Y. Han, B. Özyilmaz, Y. Zhang, and P. Kim, *Phys. Rev. Lett.* **98**, 206805 (2007).
- <sup>2</sup>L. Tapasztó, G. Dobrik, P. Lambin, and L. P. Biró, *Nat. Nanotechnol.* **3**, 397 (2008).
- <sup>3</sup>X. Wang, Y. Ouyang, X. Li, H. Wang, J. Guo, and H. Dai, *Phys. Rev. Lett.* **100**, 206803 (2008).
- <sup>4</sup>L. Jiao, L. Zhang, X. Wang, G. Diankov, and H. Dai, *Nature (London)* **458**, 877 (2009).
- <sup>5</sup>L. Yang, M. L. Cohen, and S. G. Louie, *Nano Lett.* **7**, 3112 (2007).
- <sup>6</sup>L. Yang, C.-H. Park, Y.-W. Son, M. L. Cohen, and S. G. Louie, *Phys. Rev. Lett.* **99**, 186801 (2007).
- <sup>7</sup>D. Prezzi, D. Varsano, A. Ruini, A. Marini, and E. Molinari, *Phys. Rev. B* **77**, 041404(R) (2008).
- <sup>8</sup>Y.-Z. Ma, J. Stenger, J. Zimmermann, S. M. Bachilo, R. E. Smalley, R. B. Weisman, and G. R. Fleming, *J. Chem. Phys.* **120**, 3368 (2004).
- <sup>9</sup>G. N. Ostojic, S. Zaric, J. Kono, M. S. Strano, V. C. Moore, R. H. Hauge, and R. E. Smalley, *Phys. Rev. Lett.* **92**, 117402 (2004).
- <sup>10</sup>L. Huang, H. N. Pedrosa, and T. D. Krauss, *Phys. Rev. Lett.* **93**, 017403 (2004).
- <sup>11</sup>F. Wang, G. Dukovic, L. E. Brus, and T. F. Heinz, *Phys. Rev. Lett.* **92**, 177401 (2004).
- <sup>12</sup>A. Hagen, G. Moos, V. Talalaev, and T. Hertel, *Appl. Phys. A: Mater. Sci. Process.* **78**, 1137 (2004).
- <sup>13</sup>A. Ueda, K. Matsuda, T. Tayagaki, and Y. Kanemitsu, *Appl. Phys. Lett.* **92**, 233105 (2008).
- <sup>14</sup>Y. W. Son, M. L. Cohen, and S. G. Louie, *Phys. Rev. Lett.* **97**, 216803 (2006).
- <sup>15</sup>J. Jiang, R. Saito, Ge. G. Samsonidze, A. Jorio, S. G. Chou, G. Dresselhaus, and M. S. Dresselhaus, *Phys. Rev. B* **75**, 035407 (2007).
- <sup>16</sup>T. Ando, *J. Phys. Soc. Jpn.* **66**, 1066 (1997).
- <sup>17</sup>V. Perebeinos, J. Tersoff, and P. Avouris, *Phys. Rev. Lett.* **92**, 257402 (2004).
- <sup>18</sup>C. D. Spataru, S. Ismail-Beigi, L. X. Benedict, and S. G. Louie, *Phys. Rev. Lett.* **92**, 077402 (2004).
- <sup>19</sup>T. Ando, *J. Phys. Soc. Jpn.* **75**, 024707 (2006).
- <sup>20</sup>S. Konabe, T. Yamamoto, and K. Watanabe, *Appl. Phys. Express* **2**, 092202 (2009).
- <sup>21</sup>S. Konabe, T. Yamamoto, and K. Watanabe, *Jpn. J. Appl. Phys.* **49**, 02BD06 (2010).
- <sup>22</sup>V. Perebeinos and P. Avouris, *Phys. Rev. Lett.* **101**, 057401 (2008).
- <sup>23</sup>K. Matsuda, T. Inoue, Y. Murakami, S. Maruyama, and Y. Kanemitsu, *Phys. Rev. B* **77**, 033406 (2008).
- <sup>24</sup>R. M. Russo, E. J. Mele, C. L. Kane, I. V. Rubtsov, M. J. Theisen, and D. E. Luzzi, *Phys. Rev. B* **74**, 041405(R) (2006).
- <sup>25</sup>L. Valkunas, Y.-Z. Ma, and G. R. Fleming, *Phys. Rev. B* **73**, 115432 (2006).
- <sup>26</sup>L. Cagnet, D. A. Tsyboulski, J.-D. R. Rocha, C. D. Doyle, J. M. Tour, and R. B. Weisman, *Science* **316**, 1465 (2007).
- <sup>27</sup>Y. Murakami and J. Kono, *Phys. Rev. Lett.* **102**, 037401 (2009).
- <sup>28</sup>Y. Murakami and J. Kono, *Phys. Rev. B* **80**, 035432 (2009).
- <sup>29</sup>Y. Miyauchi, H. Hirori, K. Matsuda, and Y. Kanemitsu, *Phys. Rev. B* **80**, 081410(R) (2009).
- <sup>30</sup>Y. F. Xiao, T. Q. Nhan, M. W. B. Wilson, and J. M. Fraser, *Phys. Rev. Lett.* **104**, 017401 (2010).
- <sup>31</sup>K. Yoshikawa, K. Matsuda, and Y. Kanemitsu, *J. Phys. Chem. C* **114**, 4353 (2010).
- <sup>32</sup>G. M. Kavoulakis and G. Baym, *Phys. Rev. B* **54**, 16625 (1996).
- <sup>33</sup>F. Wang, Y. Wu, M. S. Hybertsen, and T. F. Heinz, *Phys. Rev. B* **73**, 245424 (2006).
- <sup>34</sup>F. Wang, G. Dukovic, E. Knoesel, L. E. Brus, and T. F. Heinz, *Phys. Rev. B* **70**, 241403(R) (2004).